ISSN 0021-3640, JETP Letters, 2019, Vol. 110, No. 2, pp. 133–139. © Pleiades Publishing, Inc., 2019.
Russian Text © The Author(s), 2019, published in Pis'ma v Zhurnal Eksperimental'noi i Teoreticheskoi Fiziki, 2019, Vol. 110, No. 2, pp. 118–125.

CONDENSED MATTER

μ*SR* Study of the Dynamics of Internal Magnetic Correlations in Tb(Bi)MnO_3 Multiferroic in Magnetically Ordered and Paramagnetic States

S. I. Vorob'ev[a, *], A. L. Getalov[a], E. I. Golovenchits[b], E. N. Komarov[a], S. A. Kotov[a], V. A. Sanina[b], and G. V. Shcherbakov[a]

[a] *Petersburg Nuclear Physics Institute, National Research Center Kurchatov Institute, Gatchina, 188300 Russia*
[b] *Ioffe Institute, Russian Academy of Sciences, St. Petersburg, 194021 Russia*
**e-mail: Vorobyev_SI@pnpi.nrcki.ru*

Received April 5, 2019; revised May 30, 2019; accepted June 10, 2019

The dynamics of internal magnetic correlations in $Tb_{0.95}Bi_{0.05}MnO_3$ multiferroic in the temperature range of 10–290 K has been studied. Separation into two phases with different relaxations of the polarization of muons in the basic matrix of the crystal and the phase separation regions has been detected for the first time both in a magnetically disordered state at $T < T_N = 40$ K and in a paramagnetic state in a transverse magnetic field of 290 G in a temperature range of 80–150 K. A muon ferromagnetic complex (Mn^{3+}–Mu–Mn^{4+}), where the hyperfine interaction in a muonium depolarizes a muon in a time less than 10^{-8} s, is formed at $T < 40$ K in phase separation regions containing pairs of Mn^{3+} and Mn^{4+} ions, as well as electrons that recharge them. In the matrix of the original crystal containing only Mn^{3+} ions, a muonium is formed with a broken hyperfine bond. In this case, muons are depolarized at a high rate because of their interactions with the local magnetic fields of a cycloid. At temperatures of 80–150 K, one phase in the phase separation regions constitutes approximately 50% and is characterized by long relaxation times about 10 μs (described by the Gaussian relaxation function). The other phase is formed by Mn^{3+}–Mn^{3+} correlations in the short-range magnetic order regions in the matrix of the original crystal, which are weakly sensitive to a magnetic field of 290 G.

DOI: 10.1134/S0021364019140121

1. INTRODUCTION

The $TbMnO_3$ compound is a II multiferroic, where ferroelectric ordering with the Curie temperature $T_C = 28$ K is due to cycloid magnetic ordering with the Néel temperature $T_N = 40$ K [1–3], and has the orthorhombic symmetry (space group *Pbnm*). We studied the magnetic properties of a ceramic $TbMnO_3$ multiferroic sample by the μ*SR* method in [4]. There was an abnormally strong relaxation of the muon polarization detected both at temperatures $T < T_N$ and in the paramagnetic state up to 150 K, above which the normal paramagnetic state was observed. In the temperature range of 50–150 K, we detected the separation of the sample into two phases with different asymmetries and muon relaxation rates, and this separation did not depend on the presence or absence of an external magnetic field. We attributed this separation to the presence of short-range magnetic order regions caused by strong frustrations of magnetic states in $TbMnO_3$ [2, 3].

The $TbMnO_3$ multiferroic is characterized by a strong magnetoelectric interaction at $T \le T_C$ attractive for applications. However, applications require such an interaction at a higher temperature. To achieve this goal, we prepared a $Tb_{0.95}Bi_{0.05}MnO_3$ single crystal and examined its magnetic and dielectric properties and the effect of an external magnetic field on them [5–8]. It was found that local phase separation regions containing Mn^{3+} and Mn^{4+} ions, as well as electrons recharging them, are formed in the original matrix of the $TbMnO_3$ crystal in $Tb_{0.95}Bi_{0.05}MnO_3$. These regions, which exist from the lowest to room temperatures, had multiferroic properties and were controlled by a magnetic field, demonstrating a strong magnetoelectric coupling [5–8]. In $Tb_{0.95}Bi_{0.05}MnO_3$, Bi^{3+} ions substituting Tb^{3+} ions have a significantly larger ion radius (1.31 vs. 1.18 Å at the coordination number $Z = 12$ [9]), which leads to local distortions of the lattice. In addition, Bi^{3+} ions contain separated pairs of $6s^2$ electrons, which break the central symmetry of such distortions [10]. At this substitution, in the immediate environment of Bi^{3+} ions, the formation of Mn^{4+} ions having a smaller ion radius than the initial Mn^{3+} ions (0.67 vs. 0.72 Å with the coordination number $Z = 6$

[9]) is favorable. As a result, the nearest Mn^{3+}–Mn^{4+} ion pairs and excess electrons appear in $Tb_{0.95}Bi_{0.05}MnO_3$ ($Mn^{4+} + e = Mn^{3+}$). The finite probability of tunneling of electrons between Mn^{3+}–Mn^{4+} ion pairs (double exchange [11, 12]) and noncentral local distortion near Bi^{3+} ions are responsible for the energy favorable process of concentration of such ion pairs and electrons recharging them in isolated regions whose real size and shape are determined by the Coulomb repulsion [13–15]. This gives bounded dynamically equilibrium phase separation regions with magnetic and structural distortions, as in $LaAMnO_3$ (A = Sr, Ca, Ba) [12, 16] and in RMn_2O_5 multiferroic manganites [17, 18].

At low temperatures, $Tb_{0.95}Bi_{0.05}MnO_3$ experienced the same set of phase transitions as $TbMnO_3$ in the original matrix. At $T < 40$ K, the phase separation regions were one-dimensional superlattices, and a set of ferromagnetic resonances from their isolated layers was observed [19]. Isolated phase separation regions appeared at 50 K $< T <$ 180 K and these regions formed a two-dimensional superstructure at temperatures above 180 K [5–8].

The aim of this work is to study the features of internal magnetic states in $Tb_{0.95}Bi_{0.05}MnO_3$ by the μ*SR* method in a wide temperature range of 10–290 K in the absence and presence of a magnetic field. This method allows obtaining information on the state of local internal magnetic fields and their dynamics in the positions of individual magnetic ions, near which muons stop [20]. This makes it possible to directly establish the presence of both the local phase separation regions and the original matrix of the $Tb_{0.95}Bi_{0.05}MnO_3$ crystal and study their properties. The relaxation function of the muon polarization is obtained and its parameters are determind (asymmetry, relaxation of the polarization, and muon spin precession frequency in the internal magnetic field of the sample and the external magnetic field). Separation into two phases with different dynamics of internal magnetic correlations at both $T < T_N$ and $T > T_N$ is observed in $Tb_{0.95}Bi_{0.05}MnO_3$ for the first time. This separation is due to the presence of phase separation regions existing at these temperatures. At $T < T_N$, some of the relaxing muons are depolarized because of the rapidly relaxing muon complexes (Mn^{3+}–Mu–Mn^{4+}) formed in one-dimensional superlattices of phase separation regions. A fast relaxation channel appears for the other detected muons through the formation of a muonium with a broken hyperfine bond in Mn^{3+}–Mn^{3+} pairs of the original matrix, which leads to the interaction of such muons with local magnetic fields in the spin cycloid. This channel is similar to that in pure $TbMnO_3$, both at $T < T_N$ and in the short-range order regions in the paramagnetic state [4]. A phase with the time of magnetic correlations longer than the observation time in $Tb_{0.95}Bi_{0.05}MnO_3$ at $T > T_N$ is observed for the first time in multiferroic manganites; the description of this phase requirs the Gaussian relaxation function. This phase belongs to phase separation regions. The relative amount of two phases at different temperatures is determined from the ratio of asymmetry values in these phases. The nature and dynamics of internal magnetic fields in phase separation regions $T \gg T_N$ are established. This information is important for possible applications of multiferroic local phase separation regions in spintronics and information technologies.

The results of the μ*SR* study of both $TbMnO_3$ and, particularly, doped $Tb_{0.95}Bi_{0.05}MnO_3$ are qualitatively different from those obtained for RMn_2O_5 (R = Eu, Gd) and $Eu_{0.8}Ce_{0.2}Mn_2O_5$ [21–23], as well as for $LaMnO_3$ and $La_{1-x}Ca_xMnO_3$ perovskite manganites, the closest in symmetry [24, 25]. The cited studies were mainly devoted to the relaxation of the muon polarization below the magnetic ordering temperature, and the paramagnetic state was a usual single-phase state with weak relaxation of the polarization. Narrow intense maxima of the relaxation rate were observed near the transition temperature T_N.

2. EXPERIMENT AND DATA PROCESSING METHOD

A disk $Tb_{0.95}Bi_{0.05}MnO_3$ ceramic sample with a diameter of 35 mm and a thickness of 5 mm for the study was fabricated by solid phase synthesis. The X-ray diffraction analysis indicated that the sample was single-phase and characterized by the space group *Pbnm*. The composition of the sample was determined by the X-ray fluorescence method. The sample was examined at the μ*SR* facility [26] placed at the output of the muon channel of the synchrocyclotron at the Petersburg Nuclear Physics Institute, National Research Center Kurchatov Institute (Gatchina, Russia). A muon beam with the mean momentum $p_\mu = 90$ MeV/*c* and the relative momentum FWHM $\Delta p_\mu/p_\mu = 0.02$ had the longitudinal polarization $P_\mu = 0.90$–0.95. The sample under study was placed in a blowing thermostat, which allowed setting the temperature with an accuracy of about 0.1 K in the temperature range of 10–290 K. The external magnetic field on the sample was created by Helmholtz coils with a stability of about 10^{-3}. The nonuniformity of the magnetic field in the sample region was estimated on a copper sample. The low relaxation rate (0.0053 ± 0.0035) μs^{-1} of the polarization of muons stopped in the copper sample indicated that the magnetic field in the sample volume was quite uniform. The time spectra of the positrons from the decay of muons were measured simultaneously in two ranges (0–10 and 0–1.1 μs) with a channel price of 4.9 and 0.8 ns/channel, respectively. Experimental data (time

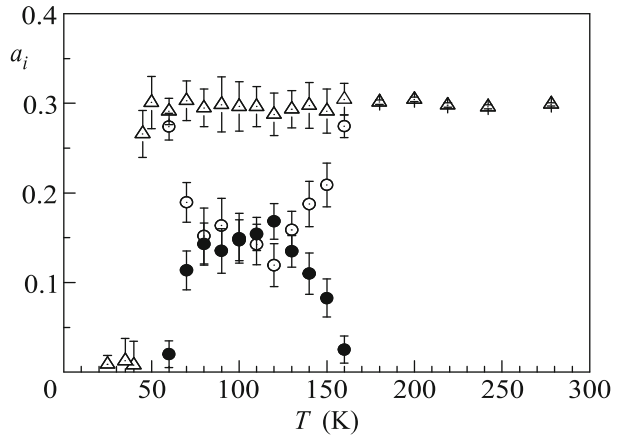

Fig. 1. Temperature dependences of the partial amplitudes of the muon spin precession in a magnetic field of H = 290 G. Open and closed circles are the amplitudes a_1 and a_2 for the phases described by Lorentzian and Gaussian relaxations, and open triangles are $a_1 + a_2$ for $T \le 160$ K and a_F for $T > 160$ K.

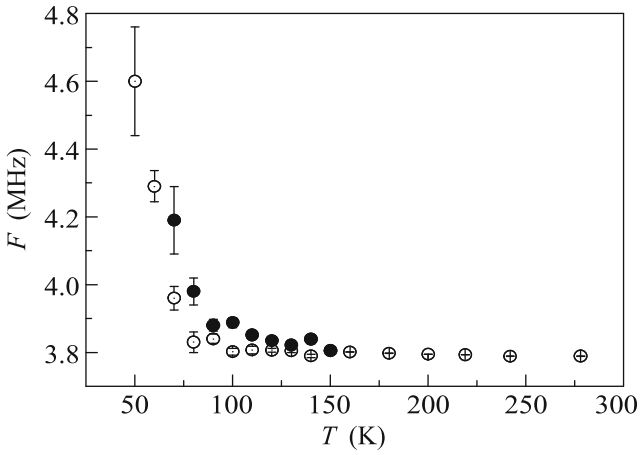

Fig. 2. Temperature dependences of the frequencies of muon spin precession (open circles) F_1 and (closed circles) F_2 in a magnetic field of H = 290 G.

positron spectra $N(t)$) were approximated by the function

$$N(t) = N_0 \exp(-t/\tau_\mu)[1 + aG(t) + a_bG_b(t)] + B, \quad (1)$$

where N_0 is the normalization constant; $\tau_\mu = 2.197$ μs is the muon lifetime; a_b and $G_b(t)$ are the fraction of the structural background and its time dependence, respectively; and B is the background of random coincidences. The technique for determining a_b, B, and $G_b(t)$ is described in detail in [22]. The parameter a depends on the initial polarization of stopped muons. The form of the time function $G(t)$ is determined by the conditions of measurements and the temperature of the sample.

Thus, the best description of the time spectra measured for $Tb_{0.95}Bi_{0.05}MnO_3$ in a paramagnetic state in a temperature range of 70–150 K in an external magnetic field of H = 290 G perpendicular to the initial spin of the muon was obtained under the assumption of a two-phase state of the sample:

$$aG(t) = a_1 \exp(-\lambda_1 t)\cos(2\pi F_1 t) + a_2 \exp[-(\lambda_2 t)^2]\cos(2\pi F_2 t). \quad (2)$$

Here, a_1 and a_2 are the partial amplitudes of the muon spin precession, which characterize the ratio of phases with the frequencies of the muon spin precession F_1 and F_2 in the external magnetic field and with the relaxation rates of the muon polarization λ_1 and λ_2. At the same time, the exponential time dependences of the relaxation function of muons in Eq. (2) had to be taken in the form of a Lorentzian and Gaussian, respectively [27]. At temperatures $T > 160$ K, a good description for the true single-phase paramagnetic state is achieved in the form

$$aG(t) = a_F \exp(-\lambda_F t)\cos(2\pi F t), \quad (3)$$

where a_F, λ_F, and F are the amplitude, relaxation rate, and muon spin precession frequency in the external magnetic field, respectively.

The processing results are shown in Figs. 1–3. Figure 1 shows not only the parameters a_1, a_2, and a_F but also the sum $a_1 + a_2$ by the same symbols as the parameter a_F. In the paramagnetic state, the sum $a_1 + a_2$ and the parameter a_F for the ceramic sample should be 0.3 [20], which is indeed the case (Fig. 1). Figure 2 shows the frequencies of the muon spin precession F_1 and F_2,

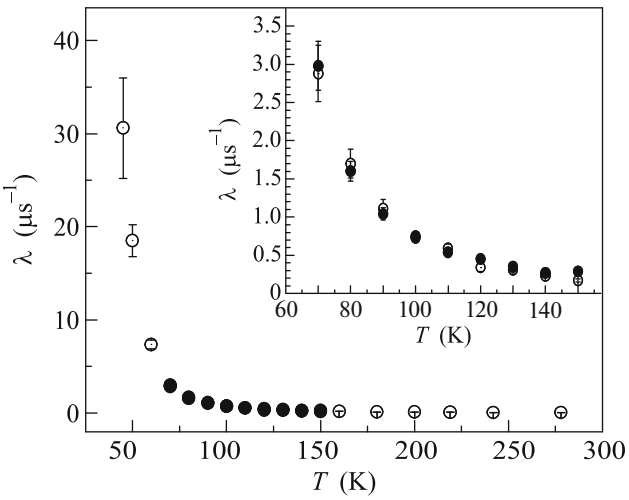

Fig. 3. Temperature dependence of the relaxation rates of the muon polarization (open circles) λ_1 and (closed circles) λ_2 in a magnetic field of H = 290 G.

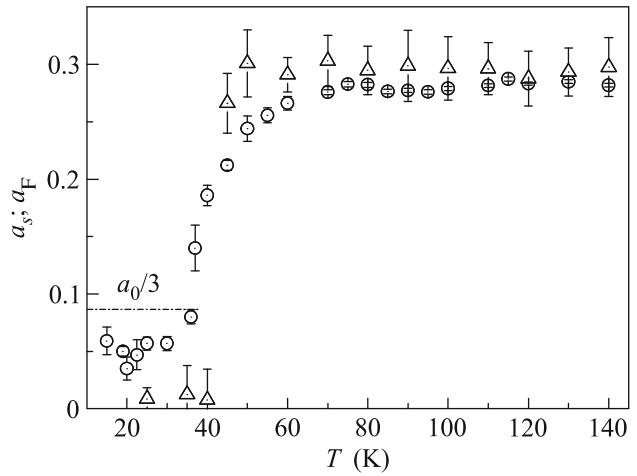

Fig. 4. Temperature dependence of asymmetries (open circles) a_s and (closed circles) a_F in a magnetic field of H = 290 G.

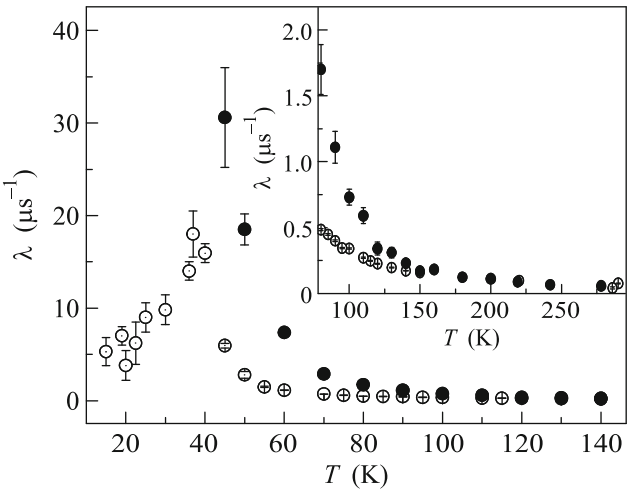

Fig. 5. Temperature dependence of the relaxation rates of the muon polarization (open circles) λ_s in zero magnetic field and (closed circles) λ_F in a magnetic field of H = 290 G.

which are slightly different at $T < 150$ K. Figure 3 shows the temperature dependences of the parameters λ_1 and λ_2, which in a magnetic field of 290 G were similar in the temperature range of 50–150 K.

Time spectra measured in zero external magnetic field were processed according to the formulas

$$aG(t) = a_s \exp(-\lambda_s t) \quad (4)$$

for sample temperatures $T > T_N = 40$ K and

$$aG(t) = as[1/3 + 2/3\cos(2\pi Ft)\exp(-\Delta t)]\exp(-\lambda_s t) \quad (5)$$

in the temperature range $T < T_N = 40$ K, where the parameters a_s and λ_s are the observed asymmetry and the relaxation rate of the muon polarization, respectively. At temperatures below T_N, the muon spin precession in the internal magnetic fields with the frequency F and standard deviation Δ is observed.

The processing results are shown in Figs. 4–7. The results in Figs. 4 and 5 are shown only for $T = 140$ K because the parameters a_s, a_F, λ_s, and λ_F hardly vary at the sample temperatures $T > 140$ K. For comparison, the same figures show the processing results for a magnetic field of 290 G. The inset of Fig. 5 shows in more detail the behavior of the parameters λ_s and λ_F in the temperature range of 75–290 K. It can be seen that the difference between the parameters λ_s and λ_F is absent at the sample temperatures above 150 K.

3. DISCUSSION OF EXPERIMENTAL RESULTS

It is noted above that the relaxation function measured in the paramagnetic state in an external magnetic field in a temperature range of 70–150 K is split into two components with different relaxation types (Lorentzian and Gaussian) of the muon polarization on the internal local magnetic fields. Lorentzian relaxation is associated with the effect of local fields with high dynamics on the muon, when $\tau_c \ll t$, where τ_c is the correlation time of the magnetic moment of the muon with these fields and t is the measurement (observation) time. In this case, the polarization relaxation rate is determined as $\lambda_1 = \sigma^2 \tau_c$ [27], where σ is the parameter of the distribution of magnetic fields in the sample. In this case, the polarization relaxation function has a Gaussian form $\exp(-\sigma^2\tau_c t) \equiv \exp(-\lambda_1 t)$. In the second case, where $\tau_c \geq t$, the relaxation function has the form $\exp(-\sigma^2 t^2) \equiv \exp(-(\lambda_2 t)^2)$ [27]. Figure 1 demonstrates that the amplitudes of the muon spin precession a_1 and a_2 with relaxation rates λ_1 and λ_2, respectively, in the temperature range of 80–150 K in the external magnetic field of H = 290 G are approximately equal to each other (each about 50%). This means that two types of sources of the local magnetic field with significantly different dynamics exist in approximately equal amounts in the sample in the external magnetic field in this temperature range. In the absence of the external magnetic field, all sources of the local magnetic field have the same dynamics (Fig. 5). Short-range magnetic order regions in the original crystal matrix containing Mn^{3+}–Mn^{3+} ion pairs, as well as phase separation regions containing Mn^{3+}–Mn^{4+} ion pairs and electrons recharging them, can serve as sources of local internal magnetic fields in $Tb_{0.95}Bi_{0.05}MnO_3$ at 80–150 K. The character of correlations of the magnetic moment of the muon with the internal fields of these pairs in two phases depends on the temperature of the sample differently, and their responses to the applied magnetic field are different. The short-range magnetic order regions in the matrix

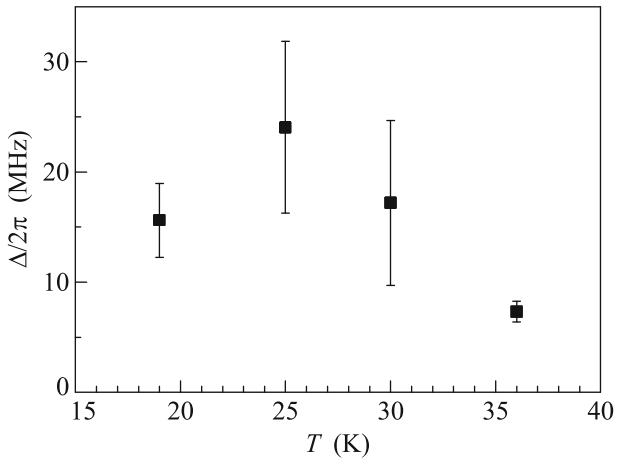

Fig. 6. Temperature dependence of the standard deviation Δ in zero magnetic field.

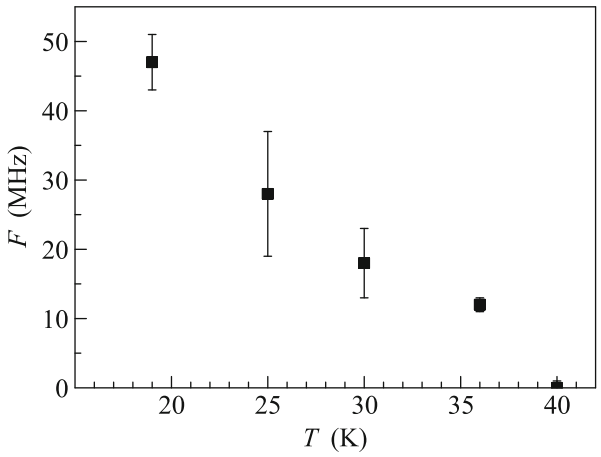

Fig. 7. Temperature dependence of the muon spin precession frequency F in zero magnetic field.

of the original crystal have strong internal magnetic fields whose state weakly depends on a magnetic field of 290 G (see Figs. 4 and 5 for $TbMnO_3$ in [4]). The relaxation of the muon polarization in such regions has a Lorentzian shape. At the same time, ferromagnetic correlations of are characteristic of phase separation regions at all temperatures. At temperatures 80 K $< T <$ 150 K, phase separation regions are isolated, and the ferromagnetic moments of Mn^{3+}–Mn^{4+} ion pairs in zero field are disoriented. When the field $H = 290$ G is applied, these moments are oriented along the field. This strongly increases the probability of electron transfer between phase separation regions in the case of their hopping conductivity by double charge exchange, increasing the correlation between them. Studies of the dielectric and magnetic properties of $Tb_{0.95}Bi_{0.05}MnO_3$ at these temperatures [5–8] showed that the application of the external magnetic field led to residual long-term effects and temperature hysteresis of states of local phase separation regions. The relaxation of the muon polarization in these regions has a Gaussian form. Thus, we can conclude that an external field of 290 G in the temperature range of 80–150 K weakly affects the states of the short-range magnetic (mostly antiferromagnetic) order in the original matrix (which was typical of pure $TbMnO_3$ [4]) and significantly affects the phase separation regions with ferromagnetic correlations, which coexist in $Tb_{0.95}Bi_{0.05}MnO_3$ with the short-range order regions in equal ratios (Fig. 1). Consequently, Mn^{3+} and Mn^{4+} ions constitute fractions of 3/4 and 1/4, respectively, in $Tb_{0.95}Bi_{0.05}MnO_3$ in the ideal variant when the phase separation regions contain only Mn^{3+}–Mn^{4+} ion pairs and the original matrix contains only Mn^{3+} ions. As mentioned above, the phase separation regions are formed near Bi^{3+} ions substituting Tb^{3+} ions. Bi^{3+} ions that are large in size and contain separated pairs of $6s^2$ electrons are responsible for structural distortions not only in the immediate environment. In this case, Mn^{4+} ions can substitute Mn^{3+} ions on a length of several lattice constants. Correspondingly, the number of appearing Mn^{4+} ions can significantly exceed the concentration of Bi^{3+} ions (5%).

Structural distortions caused by Bi^{3+} ions and by the partial substitution of Mn^{4+} ions for Mn^{3+} ions also occur in phase separation regions in the temperature range 80 K $< T <$ 150 K. It is noteworthy that changes in the lattice parameters were observed in $Tb_{0.95}Bi_{0.05}MnO_3$ single crystals in neutron diffraction studies in this temperature range in [28].

It is important to note that the sum of the partial amplitudes $a_1 + a_2$ is equal to a_F for all the temperatures of the studied sample above the Néel temperature (Fig. 4). This indicates that no other relaxation channels of polarization other than the ones indicated above exist in the temperature range 80 K $< T <$ 150 K.

In the region of critical fluctuations, in the temperature range 40 K $< T <$ 70 K, the frequencies of the muon spin precession (Fig. 2), as well as the polarization relaxation rates (Fig. 3), increase noticeably for both phases: the short-range order regions of the original matrix, which are slightly sensitive to the field H, and the phase separation regions, which are oriented by the magnetic field. In Figs. 4 and 5, the asymmetry parameter a_s and relaxation rate λ_s (at $H = 0$) refer to the short-range order regions, whereas the parameters a_F and λ_F (at $H = 290$ G) refer to the phase separation regions.

The comparative analysis of the temperature dependences of the parameters λ_s and λ_F (Fig. 5) shows that these parameters are the same in the temperature range of 150–290 K, and the difference between them appears below $T = 150$ K. The difference $\lambda_F - \lambda_s$ increases with a decrease in the sample

temperature (Fig. 5). This can be due to the effect of the external magnetic field on the dynamics of the sources of local magnetic fields. Weakening of the dynamics of local fields leads to an increase in τ_c, which in turn increases λ_F. Note that the weakening of the dynamics in the applied magnetic field refers to both phase separation regions and short-range order regions. First, the formation of one-dimensional superlattices with ferromagnetic layers begins when the temperature approaches 70 K; these superlattices also exist at $T < T_N$ [16]. Second, the short-range order regions are enlarged and their properties approach those observed in $TbMnO_3$ at $T < T_N$ [4].

A magnetically disordered state occurs in the $Tb_{0.95}Bi_{0.05}MnO_3$ sample below the temperature T_N = 40 K. The asymmetry a_s observed in zero field was significantly lower than an expected value of $a_0/3$ (Fig. 4). Muons lose polarization; we attribute this process to the appearance of an additional rapid muon depolarization channel. A rapidly relaxing muonium atom $Mu = \mu^+e^-$ is formed when the muon stops near Mn^{3+}–Mn^{4+} pairs between which e_g electrons are transferred at double exchange. In this case, muons bind these electrons, forming Mu atoms. The polarization of such muons relaxes in a time less than the time resolution of the facility. Thus, the loss of polarization occurs when muons stop in phase separation regions. This effect was previously observed in RMn_2O_5 samples [21–23], which are characterized by the formation of phase separation regions. The qualitative difference in the relaxation of muons in the phase separation regions in magnetically disordered and paramagnetic (in the applied magnetic field) states is remarkable. At $T < 40$ K, phase separation regions are one-dimensional superlattices, where the tunneling conduction mechanism prevails and e_g electrons are predominantly concentrated within phase separation regions.

In this case, the probability of the formation of rapidly relaxing muonium atoms is maximal, which leads to the loss of polarization. The hopping conduction between isolated phase separation regions oriented by the magnetic field prevails in the temperature range of 80–150 K. This increases the correlation between these regions through double exchange, significantly slowing the relaxation of muons.

A muon channel of polarization relaxation of a different nature occurs when muons stop near pairs of the same valence manganese ions (Mn^{3+}–M^{3+}) in the original $Tb_{0.95}Bi_{0.05}MnO_3$ matrix. The muon alternately interacts with two e_g electrons of these ions, whose spins make an angle of $\Theta = 0.28\pi$ [3].

The double exchange between neighboring Mn^{3+}–M^{3+} ions ($J_{de} = t\cos(\Theta/2)$) is weakened slightly in the cycloid compared to the ferromagnetic state ($\cos(\Theta/2) \approx 0.9$) and a quasimuonium can be formed. The characteristic frequency for double exchange with $J_{de} \approx 270$ MeV is $\nu = 6.6 \times 10^{13}$ Hz. The hyperfine splitting frequency in the free muonium atom is $\nu_0 = \omega_0/2\pi \approx 4.46 \times 10^9$ Hz. In the case of a fast exchange, when $\nu \gg \nu_0$, the hyperfine bond in the muonium is broken; the direct interaction of the muon spins with the internal magnetic fields of the cycloid appears. The high frequency of reorientation of e_g electron spins at the appearance and disappearance of the hyperfine interaction in the muonium leads to the exponential relaxation of the longitudinal polarization of muons. The following expression was obtained for the relaxation rate λ_s of the longitudinal component at $\nu \gg \nu_0$ [20, 29]:

$$\lambda_s = (\omega_0^*)^2/4\nu, \quad (6)$$

where ω_0^* is the hyperfine splitting frequency of the muonium in the medium and ν is the frequency of reorientation of the electron spin in the muonium.

Figure 5 demonstrates that the relaxation rate λ_s decreases from 15 to 5 μs^{-1} as the temperature decreases in the temperature range of the magnetically ordered state of the sample. This corresponds to a change in the exchange frequency from 1.2×10^{13} to 3.6×10^{13} Hz (the characteristic double-exchange frequency is $\nu = 6.6 \times 10^{13}$ Hz). The calculation by Eq. (6) was performed under the assumption that $\omega_0^* = \omega_0$, while the hyperfine splitting frequency of muonium in the medium can be less than that in vacuum ($\omega_0^* \le \omega_0$). A similar mechanism of relaxation of muons was observed in $TbMnO_3$ [4] in a magnetically disordered state and in the temperature range of the existence of short-range magnetic order regions. This depolarization mechanism is observed in about 50% of muons stopped in the $Tb_{0.95}Bi_{0.05}MnO_3$ sample (Fig. 4). The second half of the muons relax in phase separation regions with loss of polarization.

The muon spin precession frequency is observed in the transverse component of the relaxation function in the local fields of the cycloid with a large standard deviation (Figs. 6 and 7). As the temperature decreases, the frequency increases, and the standard deviation remains quite large and hardly changes in the entire temperature range below the temperature T_N.

4. CONCLUSIONS

The μSR study of the $Tb_{0.95}Bi_{0.05}MnO_3$ multiferroic has revealed a number of features that were not observed in the study of other multiferroic manganites, including $TbMnO_3$. In particular, the sample subjected to a weak magnetic field of about 300 G is separated into two fractions in the dynamics of internal magnetic correlations in the temperature range of 80–150 K. In one fraction (50% of the sample) attributed to phase separation regions, the lifetime of

correlations exceeds the measurement time (10 μs). Phase separation is caused by the appearance of Mn^{3+} and Mn^{4+} ions in the sample doped with Bi^{3+} ions. The second fraction in the same temperature range is formed by the Mn^{3+}–Mn^{3+} correlations in the short-range magnetic order regions in the matrix of the original crystal, which is slightly sensitive to a magnetic field of 290 G. This state was observed previously in $TbMnO_3$.

Two muonium relaxation channels of the muon polarization have been observed in the temperature range $T < T_N = 40$ K of the magnetically disordered state. The first channel is associated with the formation of muon ferromagnetic complexes (Mn^{3+}–Mu–Mn^{4+}) in phase separation regions. In these complexes, the muon loses polarization because of the hyperfine interaction in the muonium in a time less than 10^{-8} s. The second channel is due to the formation of quasimuonium with the broken hyperfine bond in the original matrix of the sample. In this case, the polarization relaxation rate is high, but the muon remains quasifree when interacting with the local magnetic fields of the cycloid. The contributions to the depolarization of muons in these two channels are approximately the same.

FUNDING

V.A. Sanina and E.I. Golovenchits acknowledge the partial support of the Presidium of the Russian Academy of Sciences (project "Actual Problems of Low Temperature Physics").

REFERENCES

1. T. Kimura, T. Goto, H. Shintani, K. Ishizaka, and Y. Tokura, Nature (London, U.K.) **426**, 55 (2003).
2. N. Aliouane, O. Prokhorenko, R. Feyerherm, M. Mostovoy, J. Strempfer, K. Habicht, K. C. Rule, E. Dudzik, A. U. B. Wolter, A. Maljuk, and D. N. Argyriou, J. Phys.: Condens. Matter **20**, 434215 (2008).
3. S. Picozzi, K. Yamauchi, I. A. Sergienko, C. Sen, B. Sanyal, and E. Dagotto, J. Phys.: Condens. Matter **20**, 434208 (2008).
4. D. S. Andrievskii, S. I. Vorob'ev, A. L. Getalov, E. I. Golovenchits, E. N. Komarov, S. A. Kotov, V. A. Sanina, and G. V. Shcherbakov, JETP Lett. **106**, 295 (2017).
5. E. I. Golovenchits and V. A. Sanina, JETP Lett. **81**, 509 (2005).
6. E. I. Golovenchits and V. A. Sanina, JETP Lett. **86**, 190 (2006).
7. V. A. Sanina, E. I. Golovenchits, and V. G. Zalesskii, Phys. Solid State **50**, 913 (2008).
8. V. A. Sanina, E. I. Golovenchits, and V. G. Zalesskii, Phys. Solid State **50**, 922 (2008).
9. R. D. Shannon, Acta Crystallogr. A **32**, 751 (1976).
10. N. A. Hill and K. M. Rabe, Phys. Rev. B **59**, 8759 (1999).
11. P. G. de Gennes, Phys. Rev. **118**, 141 (1960).
12. L. P. Gor'kov, Phys. Usp. **41**, 581 (1998).
13. C. Ortix, J. Lorenzana, and C. di Castro, Phys. Rev. Lett. **100**, 246402 (2008).
14. C. Ortix, J. Lorenzana, and C. di Castro, J. Phys.: Condens. Matter **20**, 434229 (2008).
15. K. I. Kugel, A. L. Rakhmanov, A. O. Sboychakov, and F. V. Kusmartsev, Semicond. Sci. Technol. **22**, 014007 (2009).
16. M. Yu. Kagan and K. I. Kugel', Phys. Usp. **44**, 553 (2001).
17. V. A. Sanina, E. I. Golovenchits, V. G. Zalesskii, S. G. Lushnikov, M. P. Scheglov, S. N. Gvasaliya, A. Savvinov, R. S. Katiyar, H. Kawaji, and T. Atake, Phys. Rev. B **80**, 224401 (2009).
18. V. A. Sanina, E. I. Golovenchits, V. G. Zalesskii, and M. P. Scheglov, J. Phys.: Condens. Matter **23**, 456003 (2011).
19. V. A. Sanina, E. I. Golovenchits, and V. G. Zalesskii, J. Phys.: Condens. Matter **24**, 346002 (2012).
20. V. P. Smilga and Yu. M. Belousov, *Muon Method in Science, Horizons in World Physics* (Nauka, Moscow, 1991; Nova Science, Commack, NY, 1994).
21. S. I. Vorob'ev, E. I. Golovenchits, V. P. Koptev, E. N. Komarov, V. P. Koptev, S. A. Kotov, V. A. Sanina, and G. V. Shcherbakov, JETP Lett. **91**, 512 (2010).
22. S. I. Vorob'ev, A. L. Getalov, E. I. Golovenchits, E. N. Komarov, V. P. Koptev, S. A. Kotov, I. I. Pavlova, V. A. Sanina, and G. V. Shcherbakov, Phys. Solid State **55**, 466 (2013).
23. S. I. Vorob'ev, D. S. Andrievskii, S. G. Barsov, A. A. Getalov, E. I. Golovenchits, E. N. Komarov, S. A. Kotov, A. Yu. Mishchenko, V. A. Sanina, and G. V. Shcherbakov, J. Exp. Theor. Phys. **123**, 1017 (2016).
24. R. H. Heffner, J. E. Sonier, D. E. MacLaughlin, G. J. Nieuwenhuys, G. Ehlers, F. Mezei, S.-W. Cheong, J. S. Gardner, and H. Roder, Phys. Rev. Lett. **85**, 3285 (2000).
25. R. H. Heffner, J. E. Sonier, D. E. MacLaughlin, G. J. Nieuwenhuys, G. M. Luke, Y. J. Uemura, W. Ratcliff, S. W. Cheong, and G. Balakrishnan, Phys. Rev. B **63**, 094408 (2001).
26. S. G. Barsov, S. I. Vorob'ev, V. P. Koptev, S. A. Kotov, S. M. Mikirtych'yants, and G. V. Shcherbakov, Instrum. Exp. Tech. **50**, 750 (2007).
27. V. A. Grebinnik, I. I. Gurevich, V. A. Zhukov, A. P. Manich, E. A. Meleshko, I. A. Muratova, B. A. Nikol'skii, V. I. Selivanov, and V. A. Suetin, Sov. Phys. JETP **41**, 777 (1975).
28. I. V. Golosovsky, A. A. Mukhin, V. Yu. Ivanov, S. B. Vakhrushev, E. I. Golovenchits, V. A. Sanina, J.-U. Hoffmann, R. Feyerherm, and E. Dudzik, Eur. Phys. J. B **85**, 103 (2012).
29. A. N. Belemuk, Yu. M. Belousov, and V. P. Smilga, J. Exp. Theor. Phys. **84**, 402 (1997).

Translated by R. Tyapaev